Angewandte
Eine Zeitschrift der Gesellschaft Deutscher Chemiker
Chemie

Supporting Information

DNA Films Containing the Artificial Nucleobase Imidazole Mediate Charge Transfer in a Silver(I)-Responsive Way

J. Christian Léon[+], Zhe She[+], Ajar Kamal, Mohtashim Hassan Shamsi, Jens Müller, and Heinz-Bernhard Kraatz**

anie_201700248_sm_miscellaneous_information.pdf

Author Contributions

J.M., H.B.K. Conceptualization: Lead; Funding acquisition: Lead; J.C.L., Z.S., A.K., M.H.S. Investigation: Lead; Project administration: Lead; J.M., H.B.K. Resources: Lead; J.M., H.B.K. Supervision: Lead; J.M., H.B.K. Validation: Lead; J.M., H.B.K. Writing—original draft: Lead; J.M., H.B.K. Writing—review & editing: Lead.

Experimental Section

Materials and reagents. Sulfuric acid (98%), sodium hydroxide, silver nitrate and potassium nitrate were obtained from Caledon (Georgetown, ON). Hydrogen peroxide (30%), 3-(*N*-morpholino)propanesulfonic acid, agar, sodium perchlorate, potassium ferrocyanide and potassium ferricyanide were bought from Sigma-Aldrich (Oakville, ON). Alumina powders (0.3 µm and 0.05 µm, respectively) were obtained from Allied High Tech Product (Compton, CA). All solutions were prepared in deionized water. Gold/Silicon (Au/Si) was prepared by the Nanofabrication facility at University of Western Ontario (London, ON). Potassium ferrocyanide and sodium perchlorate was purchased from Sigma-Aldrich (Oakville, ON). All aqueous solutions were prepared using deionized water (Millipore Milli-Q; 18 MΩcm resistivity). The reagents were used as received. Milli-Q water was used throughout this study for all purposes including electrochemistry, sample solutions and rinsing.

The **synthesis of the imidazole nucleoside** has been reported elsewhere[1], while phosphoramidites of the canonical nucleosides were purchased from Glen Research. **Oligonucleotide synthesis** and purification were performed as described previously.[2] The concentrations of oligonucleotide solutions were determined based on their absorbance. Desalted oligonucleotides were characterized by MALDI-ToF mass spectrometry (ODN1: calcd. for $[M+H]^+$: 8277 Da, found: 8277 Da; ODN2: calcd. for $[M+H]^+$: 7985 Da, found: 7981 Da; ODN3: calcd. for $[M+H]^+$: 8219 Da, found: 8218 Da; ODN4: calcd. for $[M+H]^+$: 7918 Da, found: 7914 Da; ODN5: calcd. for $[M+H]^+$: 8103 Da, found: 8103 Da; ODN6: calcd. for $[M+H]^+$: 7784 Da, found: 7786 Da; ODN7: calcd. for $[M+H]^+$: 8103 Da, found: 8102 Da; ODN8: calcd. for $[M+H]^+$: 7784 Da, found: 7784 Da; ODN9: calcd. for $[M+H]^+$: 8103 Da, found: 8103 Da; ODN10: calcd. for $[M+H]^+$: 7784 Da, found: 7786 Da; ODN11: calcd. for $[M+H]^+$: 7784 Da, found: 7808 Da; ODN12: calcd. for $[M+H]^+$: 8103 Da, found: 8102 Da, see Table S1). MALDI-TOF mass spectra were recorded on a Bruker Reflex IV instrument by using a 3-hydroxypicolinic acid/ ammonium citrate matrix.

Spectroscopy UV and CD spectra were obtained using solutions containing 1 µM duplex, 150 mM $NaClO_4$, and 5 mM MOPS at pH 6.8. UV spectra were recorded on a CARY BIO 100 spectrophotometer. UV melting profiles were recorded from 10 °C to 70 °C (1 °C/min, data interval 0.5 °C). UV absorbance at 260 nm was normalized ($A_{norm} = (A - A_{min})/(A_{max} - A_{min})$. The maxima of the derivatives of the melting curves account for the melting temperatures. CD spectra were recorded on a Jasco J-815 spectrometer at 10 °C. After smoothing, manual baseline corrections were applied.

For **electrode fabrication**, CHI101 gold disc electrodes (radius: 1 mm) were first dipped into "Piranha" solution (98% H_2SO_4 / 30% H_2O_2 : 3/1 (v/v)) and then polished in alumina slurries (1 µm, 0.3 µm and 0.05 µm) for 3 minutes each. After sonication in Milli-Q H_2O and ethanol, electrochemical cleaning was performed first in KOH (0.5 M) from -2 to 0 V at 0.5 Vs^{-1} and then in H_2SO_4 (0.5 M) from 0 to 1.5 V at 0.5 Vs^{-1} for minimum 100 cycles each until reproducible scans were obtained. Then, the gold electrode was immersed in DNA solution (25 µM dsDNA, 150 mM $NaClO_4$, 5 mM MOPS at pH 6.8) for 4 days. To minimize any interaction of the redox probe with the gold surface by blocking the pin holes, the electrode was treated with 6-mercaptohexan-1-ol solution (1 mM MCH, 150 mM $NaClO_4$, 5 mM MOPS at pH 6.8) for 2 h. Finally, the electrode was treated with Ag(I) solution (10 µM $AgNO_3$,

150 mM $NaClO_4$, 5 mM MOPS at pH 6.8). After each step, the electrode was thoroughly washed with buffer (150 mM $NaClO_4$, 5 mM MOPS at pH 6.8).

All **electrochemical measurements** were carried out within a Faraday cage. CV, SWV and EIS measurements were performed on a CHI-6059E potentiostat (CH instruments, Austin, TX) using an electrochemical cell with a three electrode configuration consisting of a DNA modified gold electrode as a working electrode, a platinum wire as a counter electrode and a Ag/AgCl (3.0 M KCl) as a reference electrode. To prevent undesired diffusion of chloride anions into the electrolyte solution, a salt bridge filled with agar gel in 1 M KNO_3 was inserted between testing and reference KCl solutions. The aqueous electrolyte containing 2 mM $K_4[Fe(CN)_6]$/2 mM $K_3[Fe(CN)_6]$, 150 mM $NaClO_4$ (supporting electrolyte) and 5 mM 3-(*N*-Morpholino)propanesulfonic acid (MOPS, pH 6.8) was used. All EIS measurements were performed with opencircuit potentials. For EIS measurements, a frequency range from 100 000 to 0.1 Hz with an amplitude of 5 mV was applied. EIS results were evaluated by using the software ZSimpWin 2.0. The obtained impedance data are analyzed by using a modified Randles' equivalent circuit (Fig. 3a). The solution resistance (R_S) is the resistance between the gold surface and the reference electrode.[3] The solution conditions (2 mM mM $[Fe(CN)_6]^{4-}$, 5 mM MOPS, 150 mM $NaClO_4$) are kept constant to minimize variations in R_S. C_M represents the capacitance of the DNA film on surface. The constant phase element (CPE) and R_X describes the properties of MCH-diluted films.[4] Since no Warburg impedance is observed (Figure 3a), possible diffusion of the redox probe into the DNA film can be ignored. R_{CT} accounts for the resistance of the DNA films to charge transfer from the electrode to the redox probe. KOH (semiconductor grade, pellets, 99.99% trace metals basis) was obtained from Sigma (Oakville, ON). Electrochemical desorption experiments were carried out using 0.5 M KOH aqueous solutions. DNA modified electrodes were used as the working electrode. The KOH solution was purged for 20 minutes with argon before each measurement. The stripping was done using cyclic voltammetric scans, starting at the open-circuit potential (approximately at 0 V) and going down to -1.6 V at a scan rate of 0.1 V/s. The stripping peak at -0.5 V, which is known to be specific to the reductive desorption of DNA/thiol SAMs, was integrated using current over time. The total charge for the peak was obtained and converted into electron density.[5]

Electrochemical Quartz Crystal Microbalance experiment was carried out using a CHI440 instrument and crystals, which were pre-calibrated to have 7.995-MHz fundamental frequency and surface of area of 0.196 cm^2. The desorption was performed by an electrochemical stripping (linear voltammetry) in the MOPs buffer by scanning the potential down from 0 V to -1.6 V, while the frequency changes were monitored at the same time. The calculation of surface mass changes was done following Sauerbrey method.[6]

Scanning Electrochemical Microscopy.

Preparation of DNA microarrays and exposure to Ag solution. Arrayit Spotbot 3 (Sunnyvale, CA) equipped with Megasonic Wash Station was used for fabricate DNA microarrays. Corresponding DNA buffer solutions were loaded into the cells in the Arrayit microplates (Sunnyvale, CA). A mixture of deionized water/ethanol (volume ratio of 9:1) was used as the wash buffer for the 946MP2 pin (Sunnyvale, CA). The humidity in the chamber was maintained at 85%-95%. The detailed spotting conditions were: Pin configuration: 1x1, Spot spacing (center to center): 200 µm, Pre-print spots per sample: 10, Sample loading time: 10.0 s, Pre-print time: 0.0 s, Print time: 1.0 s, Number of wash/dry cycles: 5, Wash/dry duration: 3.0 s, Last cycle wash duration: 5.0 s, Last cycle dry duration: 10 s. The substrate with microarrays of DNA was placed on top of a moist filter paper by MOPS buffer (pH 6.8) inside a Petri dish for 5 days. The substrates were then removed and rinsed thoroughly using MOPS buffer and blown dried using nitrogen gas. The DNA microarrays are exposed to Ag

solution for 2 hours after SECM measurement and rinsed with MOP buffer in prior to SECM measurement on the same substrate with DNA/Ag modifications.

Scanning electrochemical microscopy measurement. SECM experiments were carried out using a CHI-900b (CH Instruments, Austin, TX) and a custom-made Pt tip. The tip was made by sealing a 25 µm dia. Pt wire (99.95%, Alfa Aesar, MA, USA) into a micropipette, which is pulled from a glass capillary 1.5/0.84 mm OD/ID (World Precision Instruments, Inc., FL, USA) using the micropipette puller (PP-83, Narishige, Japan).[7] The electrode was polished carefully to RG~5 using alumina lapping discs (3.0, 0.3 and 0.05 µm, World Precision Instruments, Inc., FL, USA). A Pt wire, an Ag/AgCl/3.0M KCl electrode, and a Pt SECM tip were fitted in as the counter electrode, reference electrode, and working electrode. Modified Au/Si substrates were mounted in the cell and used as the 2nd working electrode without any bias during the experiment. The tip was always cleaned in prior to the measurement by sonication in water/ethanol (50:50) for 10 mins and running cyclic voltammetric scans in acid (H_2SO_4, pH 1) between 0 and 1.4 V for 100 cycles at scan rate of 0.5 V/s. The MOP buffer solution (pH 6.8) for SECM measurement contains 1 mM $K_4[Fe(CN)_6]$ aqueous solution as the redox probe and 150 mM $NaClO_4$ as the supporting electrolyte. A steady current is always obtained in prior to any approach curve measurement and imaging. The imaging was carried out with 5 µm increment step (0.066667s) at an applied potential of 0.6 V. The SECM images were normalized to the background current, which was the unmodified gold surface.

COMSOL Multiphysics. The experimental approach curves were normalized to the steady-state current. The experimental curves were fitted against theoretical curves simulated using COMSOL Multiphysics software following former reported models.[7-8] Subsequently, the reaction kinetics for the modified surfaces was estimated. The continuous and dashed lines shown in the Figure S8 are calculated using known values for the dimensionless rate constant (Λ). The normalized distance (L) is the ratio of the tip/substrate separation (d/a) to the tip radius. Rate constant, k^0, plots in Figure 5c are microarray of DNA and DNA/Ag spots.

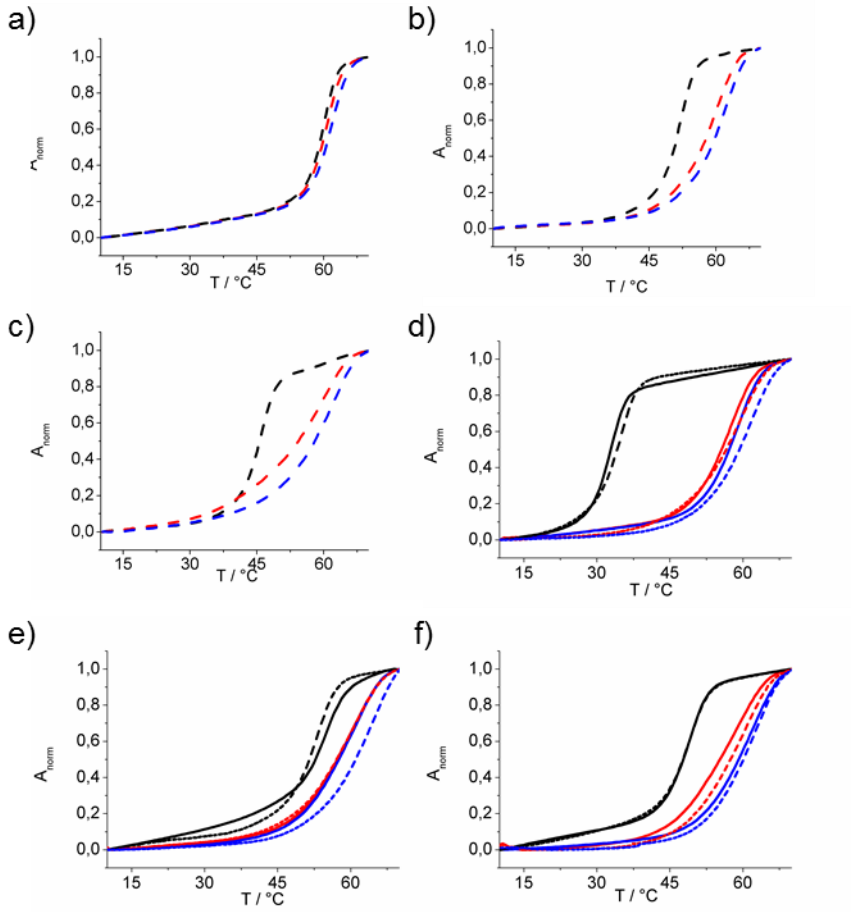

Fig. S1: UV melting profiles of duplexes in presence of increasing Ag(I) concentration. Solid lines represent melting curves of a duplex without a disulfide modification, while dashed lines represent the same duplex containing a disulfide modification. Melting profiles for duplexes analogous to **I-III** but without disulfide modification have been reported previously.[9] Black lines account for a metal-free duplex, red lines for a duplex containing 1.0 equiv. of Ag(I) with respect to number of Im:Im mispairs and blue lines for a duplex containing 1.5 equiv. of Ag(I). a) Duplex **I**: ΔT_m (without disulfide) = 0 °C, ΔT_m (with disulfide) = 1 °C; b) duplex **II**: ΔT_m (without disulfide) = 6 °C, ΔT_m (with disulfide) = 8 °C; c) duplex **III**: ΔT_m (without disulfide) = 15 °C, ΔT_m (with disulfide) = 15 °C; d) duplex **IV**: ΔT_m (without disulfide) = 25 °C, ΔT_m (with disulfide) = 26 °C; e) duplex **V**: ΔT_m (without disulfide) = 5 °C, ΔT_m (with disulfide) = 6 °C; e) duplex **VI**: ΔT_m (without disulfide) = 10 °C, ΔT_m (with disulfide) = 11 °C. Differences in ΔT_m for duplexes with and without disulfide are within the estimated error (±1 °C). Experimental conditions: 1 µM duplex, 5 mM MOPS, 150 mM $NaClO_4$, pH 6.8.

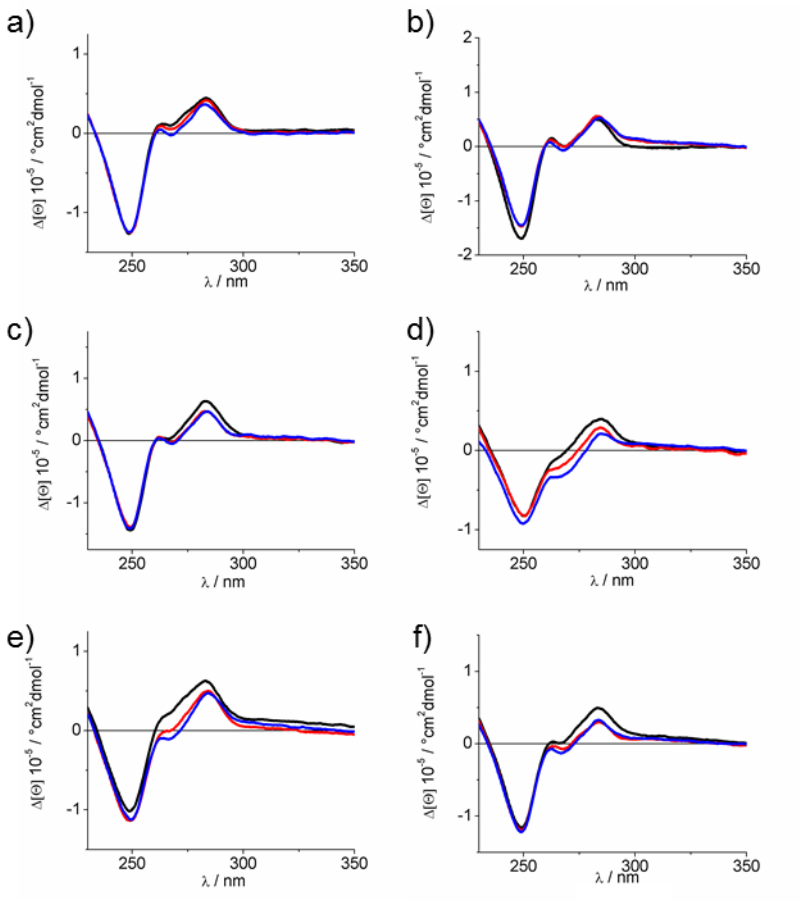

Fig. S2: CD spectra of duplexes in presence of increasing Ag(I) concentration. Black lines accounts for a metal-free duplex, red lines for a duplex in the presence of 1.0 equiv. of Ag(I) with respect to number of Im:Im mispairs and blue lines for a duplex in the presence of 1.5 equiv. of Ag(I). a) Duplex **I**; b) duplex **II**; c) duplex **III**; d) duplex **IV**; e) duplex **V**; f) duplex **VI**. All spectra show the presence of a right-handed DNA conformation throughout the experiments. Experimental conditions: 1 μM duplex, 5 mM MOPS, 150 mM $NaClO_4$, pH 6.8.

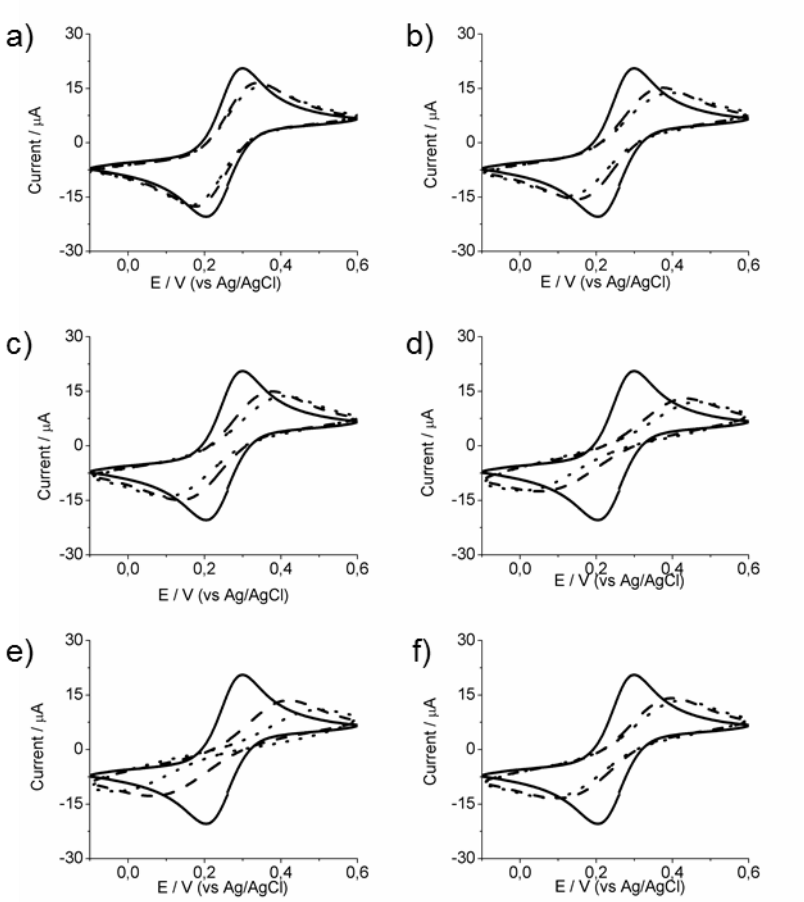

Fig. S3: Cyclic voltammograms of a gold surface (solid line) modified with duplex and MCH before (dashed line) and after incubation in a $AgNO_3$ solution (dotted line). Oxidation and reduction peaks for the unmodified gold electrode can be identified at 0.21 and 0.29 V. After being coated with duplex and MCH, the oxidation peak shifts to a more positive potential of a) duplex **I**: 0.34 V, b) duplex **II**: 0.38 V, c) duplex **III**: 0.38 V, d) duplex **IV**: 0.44 V, e) duplex **V**: 0.42 V, f) duplex **VI**: 0.40 V, while the corresponding reduction peak shifts to a) duplex **I**: 0.18 V, b) duplex **II**: 0.15 V, c) duplex **III**: 0.15 V, d) duplex **IV**: 0.04 V, e) duplex **V**: 0.6 V, f) duplex **VI**: 0.10 V. After incubation in $AgNO_3$, the oxidation peak moves to a more positive potential of a) duplex **I**: 0.35 V, b) duplex **II**: 0.40 V, c) duplex **III**: 0.41 V, d) duplex **IV**: 0.47 V, e) duplex **V**: 0.50 V, f) duplex **VI**: 0.43 V, while the reduction peak moves to a) duplex **I**: 0.17 V, b) duplex **II**: 0.12 V, c) duplex **III**: 0.10 V, d) duplex **IV**: 0.01 V, e) duplex **V**: 0.03 V, f) duplex **VI**: 0.07 V. Due to the DNA / MCH film formed on surface, electron transfer permittivity is reduced and thus, a higher overpotential is needed for the redox reaction of $[Fe(CN)_6]^{3-/4-}$. After incubation in $AgNO_3$, the oxidation peak again moves to a more positive potential while the reduction peak moves to a less positive potential. It can be concluded, that the formation of Ag(I)-mediated base pairs in the DNA film leads to a reduced electron transfer permittivity due to the increased film thickness. Experimental conditions: 2 mM $[Fe(CN)_6]^{3-}$ / 2 mM $[Fe(CN)_6]^{4-}$, 5 mM MOPS and 150 mM $NaClO_4$, pH 6.8. The cyclic voltammetry was all obtained using a start with open-circuit potential and a scan rate of 0.1 V/s.

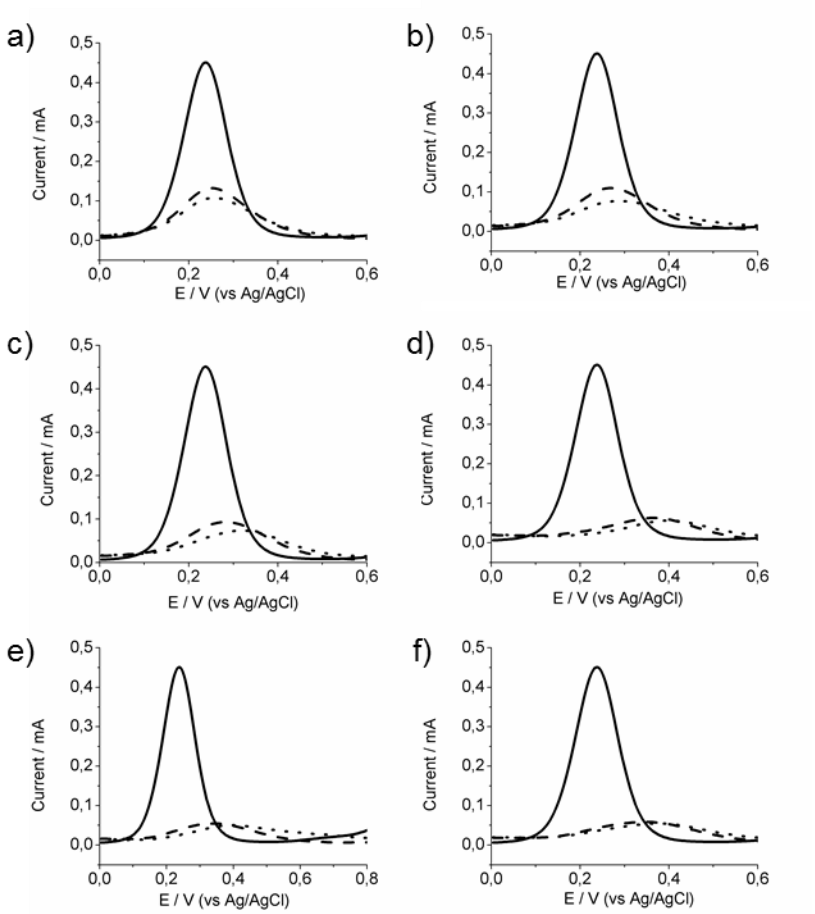

Fig. S4: Square-wave voltammograms of a gold surface (solid line) modified with duplex and MCH before (dashed line) and after incubation in a $AgNO_3$ solution (dotted line). a) duplex **I**; b) duplex **II**; c) duplex **III**; d) duplex **IV**; e) duplex **V**; f) duplex **VI**. Experimental conditions: 2 mM $[Fe(CN)_6]^{3-}$ / 2 mM $[Fe(CN)_6]^{4-}$, 5 mM MOPS and 150 mM $NaClO_4$, pH 6.8. SWV data were obtained using an amplitude of 0.025 V and a frequency of 15 Hz.

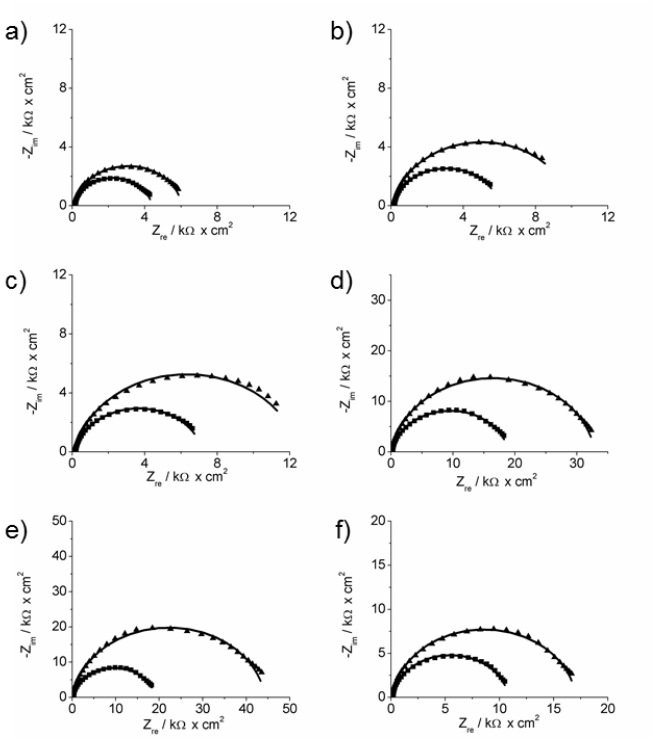

Fig. S5: Representative Nyquist plots before (■) and after (▲) incubation of a gold surface modified with a duplex in $AgNO_3$. The solid lines represent impedance curves calculated by using the circuit model shown in the inset in Figure 3a. The R_{CT} values for a) duplex **I**; b) duplex **II**; c) duplex **III**; d) duplex **IV**; e) duplex **V**; f) duplex **VI** are summarized in Table S2. Experimental conditions: 2 mM $[Fe(CN)_6]^{3-}$ / 2 mM $[Fe(CN)_6]^{4-}$, 5 mM MOPS and 150 mM $NaClO_4$, pH 6.8. A frequency range from 100 000 to 0.1 Hz with an amplitude of 5 mV was applied

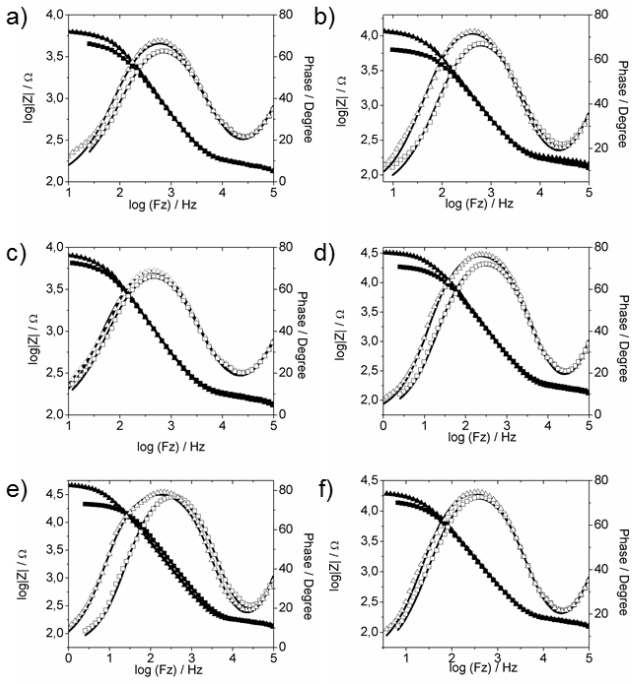

Fig. S6: Representative Bode plots: impedance magnitude (black) and phase angle (white) as a function of frequency before (■) and after (▲) incubation of a gold surface modified with a duplex in $AgNO_3$. The solid lines represent impedance curves calculated by using the circuit model shown in the inset in figure 3a. The R_{CT} values for a) duplex **I**; b) duplex **II**; c) duplex **III**; d) duplex **IV**; e) duplex **V**; f) duplex **VI** are shown in Table S2. Experimental conditions: 2 mM $[Fe(CN)_6]^{3-}$ / 2 mM $[Fe(CN)_6]^{4-}$, 5 mM MOPS and 150 mM $NaClO_4$, pH 6.8.

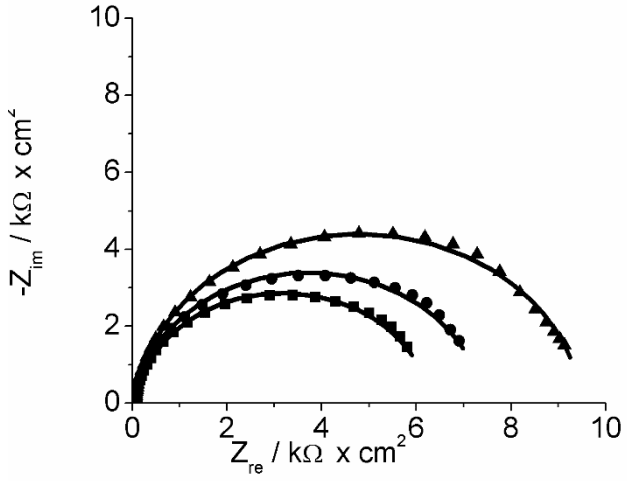

Fig. S7: Representative Nyquist plots of a gold surface covered with a film of duplex **I** before (■) and after incubation in 10 µM $LiClO_4$ solution (●) and subsequent incubation in 10 µM $AgNO_3$ solution (▲). The solid lines represent impedance curves calculated by using the circuit model shown in the inset in Figure 3a.

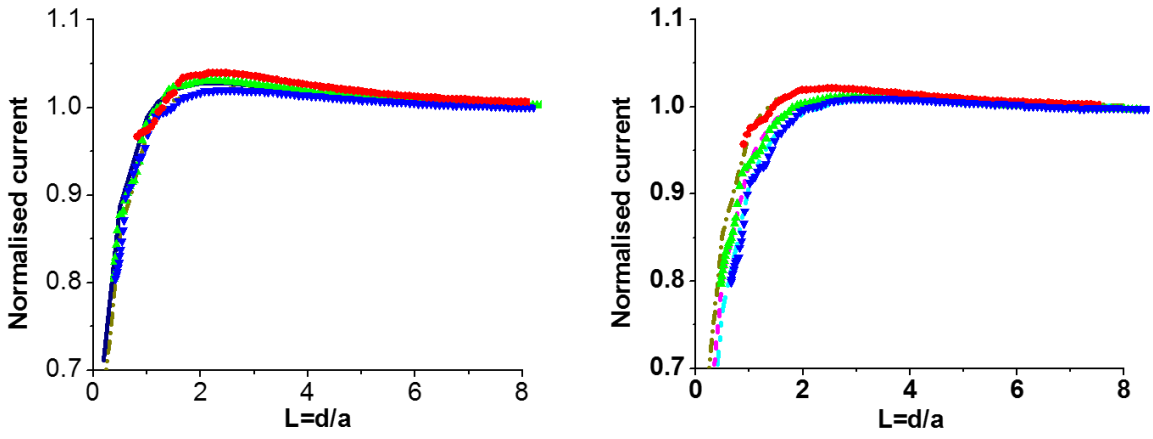

Fig. S8: Example of approach curves measured from DNA microarrays a) before and b) after exposure to Ag(I) ions using scanning electrochemical microscopy (SECM). The scatters are experimental curves of duplex **VI** (●), duplex **III** (▲), and duplex **V** (▼), which were then fitted into COMSOL Multiphysics simulated line curves. The experimental approach curves were normalized to the steady-state current. Subsequently, the reaction kinetics for the modified surfaces were estimated. The normalized distance (*L*) is the ratio of the tip/substrate separation (*d*/*a*) to the tip radius. The measurements were carried out in a MOPS buffer solution (pH 6.8) containing 1 mM $K_4[Fe(CN)_6]$ as the redox probe and 150 mM $NaClO_4$ as

the supporting electrolyte. A steady current was always obtained in prior to any approach curve measurement.

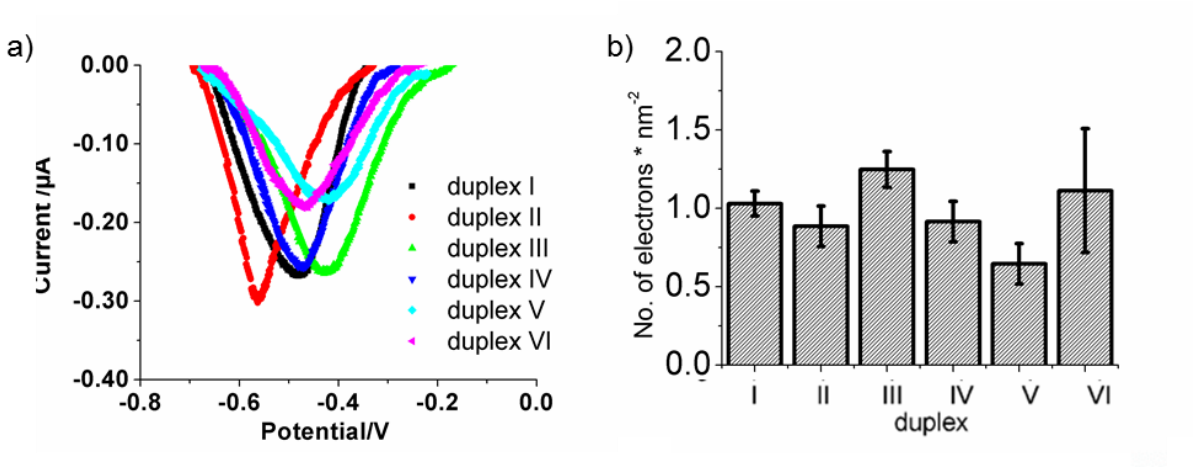

Fig. S9: a) Reductive desorption peaks for duplexes **I**-**VI** recorded in 0.5 M KOH at a rate of 0.1 Vs^{-1}. b) Electron density of the reductive desorption which was obtained by integrating the desorption peaks over time. The electron density of the individual duplexes do not appear to be significantly different.

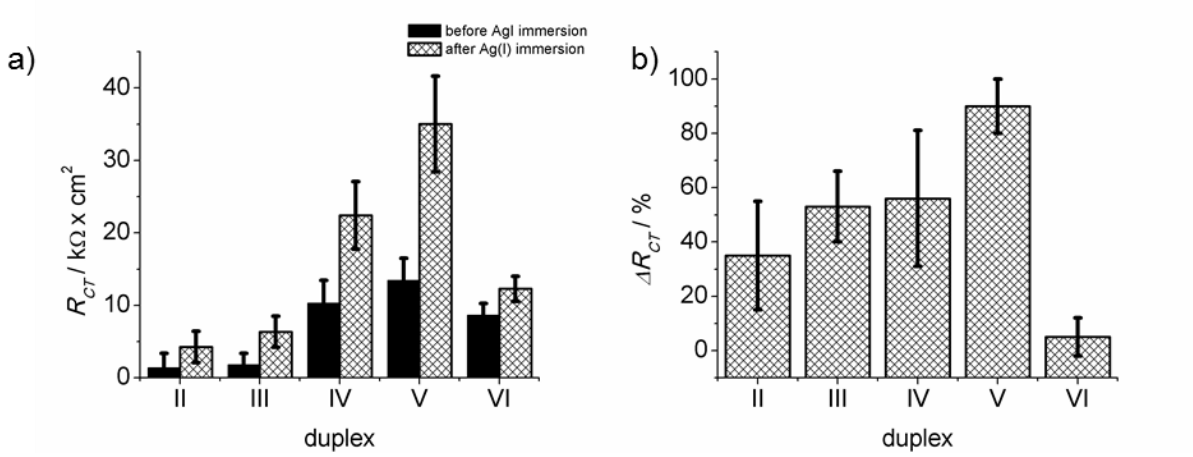

Fig. S10: a) R_{CT} values before and after incubation in 10 µM $AgNO_3$ solution and b) relative changes ΔR_{CT} in % for films of duplex **II-VI.** The data represent the average of three individual measurements. In all cases, the data of duplex **I** have been subtracted from the respective experimental data, as they represent the background signal. Error propagation was applied.

Table S1: Oligonucleotides used in this study. X = imidazole, R = $(CH_2)_6$-S-S-$(CH_2)_6$-OH.

Duplex	ODN	Sequence
I	1	R-5'-d(TTT GTT TGT TTG TTT GTT TTT TTT TT)-3'
	2	3'-d(AAA CAA ACA AAC AAA CAA AAA AAA AA)-5'
II	3	R-5'-d(TTT GTT TGT TTG T**X**T GTT TTT TTT TT)-3'

	4	3'-d(AAA CAA ACA AAC A**X**A CAA AAA AAA AA)-5'
III	5	R-5'-d(TTT GTT TGT TTG **XXX** GTT TTT TTT TT)-3'
	6	3'-d(AAA CAA ACA AAC **XXX** CAA AAA AAA AA)-5'
IV	7	R-5'-d(TTT G**X**T TGT TTG T**X**T GTT TTT **X**TT TT)-3'
	8	3'-d(AAA C**X**A ACA AAC A**X**A CAA AAA **X**AA AA)-5'
V	9	R-5'-d(TTT G**XX X**GT TTG TTT GTT TTT TTT TT)-3'
	10	3'-d(AAA C**XX X**CA AAC AAA CAA AAA AAA AA)-5'
VI	11	R-5'-d(TTT GTT TGT TTG TTT GTT T**XX X**TT TT)-3'
	12	3'-d(AAA CAA ACA AAC AAA CAA A**XX X**AA AA)-5'

Table S2: Values of the equivalent circuit elements shown in Figure 3a obtained from EIS measurements. R_S was kept constant at 0.04(1) kΩ. It should be noted that the standard deviation of the relative increase of R_{CT} appears to be smaller for systems containing three consecutive Im:Im mismatches compared to those with either a single or multiple separated but individual binding sites. This finding may be rationalized by cooperativity associated with the formation of neighboring metal-mediated base pairs.[9b, 10]

	C_M / nF	R_{CT}/kΩ	R_X/kΩ	CPE /μF	n	ΔR_{CT}/%
Duplex ***I***	7 ± 0.3	6 ± 2	0.154 ± 0.001	0.4 ± 0.2	0.90 ± 0.02	
Duplex ***I*** + Ag(I)	7 ± 0.5	7 ± 2	0.153 ± 0.001	0.5 ± 0.2	0.90 ± 0.03	33 ± 6
Duplex ***II***	9 ± 2	7 ± 1	0.152 ± 0.005	0.6 ± 0.1	0.90 ± 0.01	
Duplex ***II*** + Ag(I)	9 ± 2	12 ± 1	0.15 ± 0.02	0.5 ± 0.1	0.90 ± 0.01	70 ± 20
Duplex ***III***	7 ± 0.4	7.3 ± 0.4	0.160 ± 0.007	0.5 ± 0.1	0.90 ± 0.03	
Duplex ***III*** + Ag(I)	7 ± 0.7	14 ± 1	0.159 ± 0.006	0.5 ± 0.1	0.90 ± 0.03	90 ± 10
Duplex ***IV***	7± 0.4	16 ± 3	0.14 ± 0.04	0.4 ± 0.2	0.90 ± 0.01	
Duplex ***IV*** + Ag(I)	7 ± 0.4	30 ± 10	0.17 ± 0.02	0.4 ± 0.1	0.90 ± 0.01	90 ± 20
Duplex ***V***	7 ± 0.3	19 ± 3	0.163 ± 0.002	0.4 ± 0.1	0.90 ± 0.02	
Duplex ***V*** + Ag(I)	7 ± 0.4	42 ± 6	0.162 ± 0.004	0.4 ± 0.1	0.90 ± 0.01	123 ± 8
Duplex ***VI***	7 ± 0.5	14.2 ± 0.4	0.15 ± 0.01	0.6 ± 0.1	0.90 ± 0.03	
Duplex ***VI*** + Ag(I)	7 ± 0.3	19.5 ± 0.5	0.15 ± 0.09	0.4 ± 0.1	0.90 ± 0.01	38 ± 4

Table S3: Rate constants k^0 were calculated using the dimensionless rate constant Λ values estimated by the contrasting the experimental approach curve data against the calculated approach curve data shown in Fig. S9.

$k^0 \times 10^{-4}$ /cm s^{-1}	DNA	DNA+Ag
Bare gold	76 ± 6	74 ± 3
Duplex **VI**	3.8 ± 0.9	3.1 ± 0.5
Duplex **III**	3.4 ± 0.6	2.6 ± 0.4
Duplex **V**	2.9 ± 0.5	2.2 ± 0.4

Table S4: R_{CT} values for each step of the electrode fabrication (bare gold, after immobilization of DNA duplex, after treatment with 6-mercaptohexan-1-ol solution, after incubation in Ag(I) solution. High standard deviations before treatment with 6-mercaptohexan-1-ol (MCH) solution can be rationalized with the diffusion of the redox probe to the Au surface.

duplex	R_{CT} (bare gold) /kΩ	R_{CT} (DNA) /kΩ	R_{CT} (DNA + MCH) /kΩ	R_{CT} (DNA + MCH + Ag(I)) /kΩ
I	0.10 ± 0.01	0.7 ± 0.3	6 ± 2	7 ± 2
II	0.10 ± 0.02	1.1 ± 0.1	7 ± 1	12 ± 1
III	0.10 ± 0.02	1.8 ± 0.6	7.3 ± 0.4	14 ± 1
IV	0.10 ± 0.01	4 ± 2	16 ± 3	30 ± 4
V	0.10 ± 0.01	6 ± 4	19 ± 3	42 ± 6
VI	0.10 ± 0.01	2.8 ± 0.5	14.2 ± 0.4	19.6 ± 0.5

Table S5: Results of quartz crystal microbalance experiments performed for the same duplexes that were selected for SECM measurements. Additionally, duplex **I** was chosen as a reference.

duplex	molecules per nm^2
I	0.025
III	0.036
V	0.026
VI	0.024

[1] J. Müller, D. Böhme, P. Lax, M. M. Cerda, M. Roitzsch, *Chemistry-a European Journal* **2005**, *11*, 6246-6253.

[2] D. A. Megger, C. F. Guerra, J. Hoffmann, B. Brutschy, F. M. Bickelhaupt, J. Muller, *Chemistry-a European Journal* **2011**, *17*, 6533-6544.

[3] H. Gong, X. H. Li, *Analyst* **2011**, *136*, 2242-2246.

[4] H. Gong, T. Y. Zhong, L. Gao, X. H. Li, L. J. Bi, H. B. Kraatz, *Analytical Chemistry* **2009**, *81*, 8639-8643.

[5] G. Sanchez-Pomales, C. R. Cabrera, *Journal of Electroanalytical Chemistry* **2007**, *606*, 47-54.

[6] G. Sauerbrey, *The Use of Quartz Crystal Oscillators for Weighing Thin Layers and for Microweighing Applications*, **1959**.

[7] P. M. Diakowski, H. B. Kraatz, *Chemical Communications* **2009**, 1189-1191.

[8] M. N. Alam, M. H. Shamsi, H. B. Kraatz, *Analyst* **2012**, *137*, 4220-4225.

[9] aK. Petrovec, B. J. Ravoo, J. Müller, *Chemical Communications* **2012**, *48*, 11844-11846; bK. Schweizer, J. C. Léon, B. J. Ravoo, J. Müller, *Journal of Inorganic Biochemistry* **2016**, *160*, 256-263.

[10] aH. Torigoe, Y. Miyakawa, A. Ono, T. Kozasa, *Thermochimica Acta* **2012**, *532*, 28-35; bH. Torigoe, A. Ono, T. Kozasa, *Chemistry-a European Journal* **2010**, *16*, 13218-13225.